

# Warpage Studies of HDI Test Vehicles During Various Thermal Profiling

Gregory J. Petriccione, I. Charles Ume, Ph.D.<sup>1</sup>  
School of Mechanical Engineering  
Georgia Institute of Technology  
Atlanta, Georgia 30332  
Phone: (404) 894-7411  
charles.ume@me.gatech.edu

## ABSTRACT

New techniques and technologies involved in the miniaturization of printed wiring board (PWB) fabrication are rapidly emerging. The quality, performance, and reliability of surface mount assemblies built on these next-generation boards will depend on many factors, including thermally induced warpage. Therefore, quantitative warpage measurement is critical in new PWB assembly design evaluation, and determining overall thermal performance characteristics. Using an automated infrared reflow oven simulation system, the warpage of six bare high density interconnect (HDI) samples is measured under two different heating profiles. Out-of-plane surface displacement is measured with a non-contact shadow moiré technique and resolution enhancement method called phase-stepping. The two types of samples evaluated were built for the purpose of warpage study, where physical data could be used to validate finite element analysis (FEA) results. The warpage results obtained with the two thermal profiles will be presented.

## INTRODUCTION

As component density and downsizing of printed wiring board assemblies (PWBAs) continue to increase through emerging high density interconnect (HDI) technology, so does the need for accurate component placement in order to manufacture defect-free electronics. This miniaturization trend coupled with the growing use of surface mount technology and thin board production has forced thermally induced PWB warpage to become both a critical manufacturing and long-term reliability issue. Excessive warpage during PWB fabrication leads to misregistration, making automated component placement and insertion difficult or impossible to achieve. Warpage also impacts the PWBA end user, where resulting high residual stresses produced during PWBA usage can ultimately cause premature solder joint failure. Thus, quantitative warpage measurement is critical in new PWBA design evaluation and determining overall thermal performance characteristics.

---

<sup>1</sup> Corresponding author.

HDI is a common industry acronym with a multitude of interpretations, but in general refers to a new fabrication technique that redefines the downsizing limits of electronic assemblies. The following describes the methods and results of measuring thermally induced warpage of six bare HDI samples produced specifically with build-up technology. The specimens, manufactured for the purpose of warpage study, were tested under two different heating cycles to examine both the warpage effects of moisture and gradual heating. Measurements were performed using the phase-stepping shadow moiré technique, a high resolution non-contact method of measuring out-of-plane surface displacement.

### **HDI BUILD-UP TECHNOLOGY**

The evolution of HDI is inherently intertwined with the history and development of PWB fabrication. Manufacturers are driven by the constant challenge to produce more complex boards that are “thinner, lighter, smaller, and cheaper” [1]. Great strides in interconnection density occurred when boards first matured from single-sided to double-sided then to multilayer (M/L) designs. PWB density increases are fueled by component technology; an early example of this relationship dates back to 1963, when mounting components vertically increased circuit density [2]. This forced board fabricators to shrink circuit trace features and create more through holes per unit area with tighter tolerances and accuracy. Thirty-five years later, the same interplay holds true with surface mount technology driving present-day HDI efforts [2].

The perpetual “dilemma” faced by the PWB industry is to meet the demand for higher density board designs without appreciable cost increases. In general, interconnect density is primarily dependent on three factors: hole diameter, trace feature resolution, and construction materials. Since mechanical drilling is both a time-varying and costly process with holes sequentially produced, traditional drilling will become a cost prohibitive factor in fulfilling future small hole high density requirements [1,3]. Imaging resolution systems have limited optimization thresholds forcing massive re-investment if very fine line capabilities are to be implemented. With the ever increasing popularity and application base of PCI and PCMCIA computer cards, complex large board designs must be retooled into smaller and thinner packages. Typical materials are beginning to prove inadequate in the quest to increase layer count while decreasing overall thickness.

According to McDermott [3], one possible approach to address each of these factors is the use of emerging HDI build-up technology. With ever-increasing surface mount IC complexity, a significant obstacle in the design of commercial electronic products is accomplishing I/O escape. Board via pad diameter has not downsized proportionally with component pitch and it is obvious that miniaturized vias and pads are now mandatory for high I/O escape. A proven cost effective solution is to implement photo-defined vias using an epoxy-based liquid photoimageable dielectric. This technology can produce small

via pads, support fine line resolution, and allows multiple sequential layers with the formation of both blind and buried vias. Further advantages include thinner dielectric, a lower dielectric constant, and even increased I/O escape, as vias can drop directly below the SMT device.

McDermott [3] also explains that the photoimageable via approach is compatible with established PWB processes and product flow. It begins with either a bare double sided or M/L board (no through-holes) that is coated with the photoimageable dielectric on both sides. The board is then patterned and developed to create vias through the dielectric to the copper surface beneath. Electroless copper is then plated onto the surface followed by standard print and etch producing the desired circuit pathways. Additional layers can be built by repeating the steps to create a dense layer interconnection utilizing buried and blind vias. Designs with high via counts can be manufactured in fewer steps using photoimageable technology (almost half as many in certain cases) as compared to conventional drill and laminate techniques. Key process parameters crucial for high yields include drilled via and photodefined via registration, copper adhesion, plating quality, and dielectric thickness. Via hole size is dominated by a dielectric thickness/hole diameter aspect ratio.

Holden [1] claims that build-up technology helps solve a three-fold challenge as the electronics packaging industry constantly pushes miniaturization. Board thickness is reduced as wiring density increases, all at a lower cost than traditional fabrication methods. As many as 12 variations of build-up technologies are in use today, each differing slightly by the dielectric material used, choice of processing (e.g., plasma etching, photo forming, or laser ablation), and specific design rule values. But regardless of the technique, all of the thin insulating materials used share non-glass reinforcement properties, making via creation possible. As with any new process, build-up technology will take time to be assimilated by designers and fabricators. They will need to address issues affecting design tools (staggered vias in CAD software), electrical testing procedures (changes in test point coverage), and standards/specifications requirements.

#### **MEASUREMENT TECHNIQUE – SHADOW MOIRÉ**

Thermally induced specimen warpage is obtained using the shadow moiré technique. This non-contact full field measurement method generates a moiré pattern- a visual pattern of light and dark regions produced by the superposition of two regular motifs that geometrically interfere [8]. A fringe pattern is essentially a contour map of the surface of the specimen.

The shadow moiré technique can be performed with a relatively simple experimental setup; typical basic components consist of a light source, camera, and reference grating (Ronchi Ruling). The reference grating is a flat, thin glass such that equally spaced parallel solid lines are etched into one side. Warpage measurement resolution is a direct function of the reference grating line spacing or density

(given as lines-per-inch, lpi), where larger lpi yields finer resolution. A grating shadow, which distorts in the presence of surface warpage, is produced on the specimen when a collimated light source is directed through the reference grating. Thus, a perfectly flat specimen parallel to the plane of the grating will not yield a moiré pattern, which only appears when surface curvature (warpage) is present. Change in surface height between any two adjacent fringes is given as the reciprocal of the grating density. Observed patterns are accurately translated into specimen out-of-plane displacement through mathematical computer analysis.

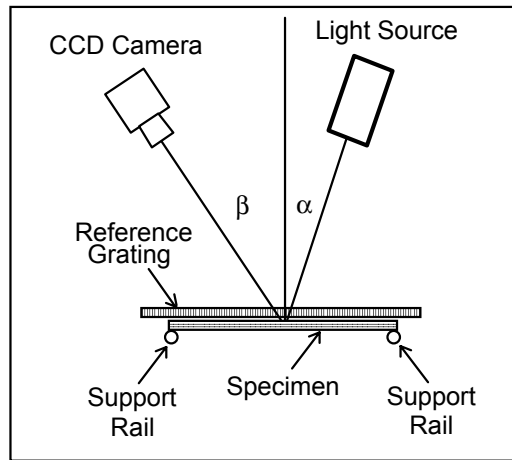


**Figure 1:** Schematic of the Shadow Moiré Setup

Setup preparation begins with horizontally supporting the specimen and suspending the reference grating directly above. As shown in **Figure 1**, the light source is directed onto the specimen through the reference grating at angle  $\alpha$  as the moiré pattern is observed by the camera at angle  $\beta$ . The out-of-plane displacement relationship is then given as:

$$\omega = (Np) / (\tan\alpha + \tan\beta)$$

where:

$\alpha$  angle of the light source with respect to the normal of the test specimen

$\beta$  angle of the camera with respect to the normal of the test specimen

$N$  fringe order or fringe count at the corresponding point

$p$  grating pitch

$\omega$  out-of-plane displacement in inches at the Nth fringe order

Choosing which grating to be used for a given experiment is based on two factors: initial specimen warpage and the maximum expected warpage. 1) Grating resolution must be smaller than initial warpage (e.g., a 100 lpi grating with 10 mil resolution will not produce fringes if the starting warpage is 7 mils.) Conversely, a denser grating for large warpage conditions produces too many fringes and makes analysis difficult. 2) A moiré pattern is produced only when the grating is a very small distance above the specimen. Although minimizing the gap between specimen and grating improves fringe contrast, it is imperative that the specimen does not touch the grating at any time during the experiment. While higher density gratings must be positioned closer to the specimen surface to maintain acceptable contrast quality, a lower density grating (which can be set farther away) is chosen if it is assumed that the specimen may undergo relatively large amounts of warpage during cycling.

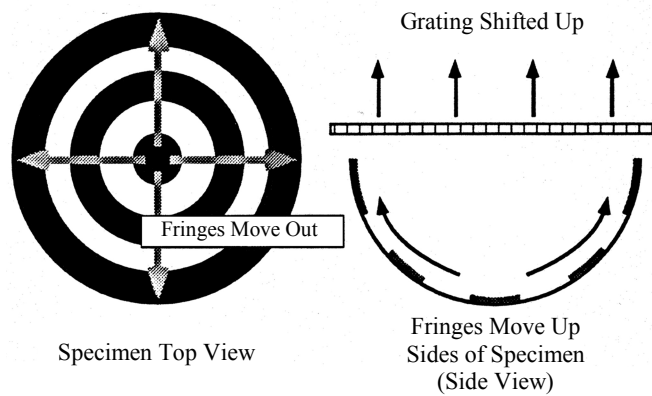


**Figure 2:** Fringe Movement Related to Grating Translation

The traditional procedure for collecting and interpreting fringe images involves capturing a single fringe pattern at each desired specimen condition as well as determining the current displacement concavity. Because a single moiré pattern alone cannot describe warpage direction, it is necessary during an experiment to temporarily raise and restore the height of the grating while observing fringe movements. As the distance between grating and specimen is increased, fringe patterns move towards “high” regions and away from “low” regions, as shown in **Figure 2**. With the concavity known, fringe ordering (counting the number of dark fringes from the specimen center to edge- see **Figure 3**) is performed to calculate out-of-plane displacement at these discrete intervals. Interpolation is then used to compute warpage along the entire surface, but the practical maximum resolution of fringe counting is always on the order of 1 mil (25  $\mu\text{m}$ ).

However, a more precise method of using moiré fringe patterns for displacement measurement is known as the phase-stepping technique. When the change in distance between the grating and specimen is a whole multiple of the grating resolution, a fringe pattern “repeats” itself, and has shifted one complete

fringe. Phase-stepping involves analyzing several fringe patterns, produced when the grating is translated a fraction of the resolution height [4,5]. This process significantly improves measurement sensitivity and inherently describes warpage direction [4,5]. Three images per measurement were used to produce the following results and increased analysis resolution by  $10^{-2}$  over traditional fringe ordering. The software algorithm used to interpret and convert the image sets into 3-D surface plots was developed by Electronic Packaging Services, Atlanta, GA.

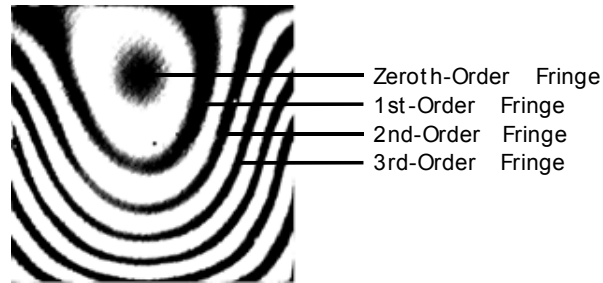


**Figure 3: Fringe Ordering**

#### **REAL-TIME WARPAGE MEASUREMENT SYSTEM**

The warpage measurement system shown in **Figure 4** has been developed at Georgia Tech's Advanced Electronic Packaging Laboratory (AEPL) and has been in use since 1994. The major system components include an infrared (IR) oven, grating/specimen positioning hardware, and central computer. Detailed information about the system setup, specifications, and components can be found in [6,7].

#### *Hardware and Software Overview*

The 5.25 cu. ft oven chamber is powered by a 5000W quartz-element IR heater. A large area glass oven top allows for the overhead viewing of fringe patterns. Desired specimen temperature, data acquisition (DAQ), and grating translation are all computer controlled. A DAQ board collects thermocouple temperature data during an experiment. Closed loop feedback control for heating is achieved with a single thermocouple placed at specimen underside center. The specimen/grating support system consists of two separate fixtures constructed with  $\frac{1}{2}$ " diameter Super Invar, a metallic alloy with a low coefficient of thermal expansion. Since the shadow moiré technique is inherently dependent on height differences between specimen and grating surfaces, Super Invar helps minimize any introduced measurement errors due to the thermal expansion of the supports. Fringe patterns are observed using a black and white CCD camera mounted above the oven chamber. Since fringe analysis is conducted after an experiment, a professional quality S-VHS video deck records the patterns generated during the run.

System-wide automation and control is performed with a highly developed virtual instrument (VI) created with a graphically-based software interface. This user interface is inherently interactive and easily manipulated with the computer keyboard and mouse. Fully tunable PID software drives the IR heaters to accurately follow most industry-standard profiles. Desired temperature profile data is manually formatted into a standard text file which lists time steps, temperature values, and grating movement instructions. Measured specimen temperatures are graphically displayed in real time along with the complete desired temperature profile curve.

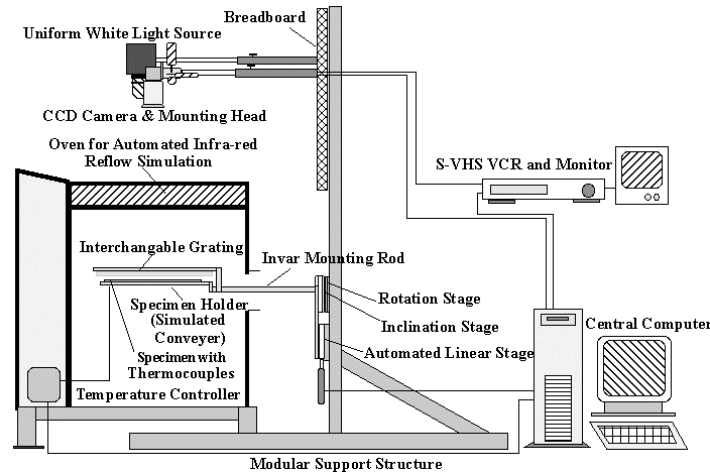


**Figure 4:** Simulated Infrared Reflow On-Line Measurement System

### *Operation Overview*

Several steps must be performed before an experiment takes place. Since moiré fringes only appear on light surfaces under adequate contrast, the sample is coated with a thin layer of white high-temperature spray paint on the side to be measured. Then, thermocouples are taped to the specimen surface at locations of interest (at least one is placed at the bottom center for feedback control). After the sample and grating are placed in the oven, the specimen is manually rotated so that its center point is parallel to the plane of the grating thus “centering” the fringes. Finally, the grating is translated close enough to the specimen so that acceptable fringe contrast is achieved.

The appropriate profile is then loaded into the VI and the VCR is set to record. During the run, the grating translates automatically as instructed in the text file during the times of interest. Manually initiated grating movements can also be performed at any time, and are necessary for measurements during unregulated cooldown. When heating is complete, the oven door is opened and the sample cools naturally or with the aid of a floor standing fan. After data collection is terminated (e.g. final room temperature,) all measurements made are saved to a text file so that the data may be plotted using

spreadsheet software. The specific images from a given run are transferred from videotape to computer using a video capture board. Image adjustments (cropping, format, size, etc.) are made using Photoshop<sup>®</sup> before phase stepping analysis is performed in Matlab 5<sup>®</sup>.

## TEST CONDITIONS

The warpage of six 3" x 3" HDI test boards was investigated using two distinct heating profiles. These specimens all share the same gold pad edge configuration, but are characterized by their solder mask color (see **Figure 5**): one three sample set is light (lt) green while the other three sample set is dark (dk) green. Specimen thickness is 30 mils and 23 mils for the light and dark green, respectively. Each set of three boards was made by a different company but came from the same batch. Board warpage was obtained using a 200 lpi reference grating; phase-stepping improved overall measurement resolution from 5 mil to 0.05 mil. The samples were simply supported along the left and right edges with 1/8" diameter Super Invar rails, which rested on the specimen support fixture. A single thermocouple at the specimen bottom center served as both the temperature driver and recorder.

One light green sample and one dark green sample were individually subjected to temperature profile 1, while the remaining 4 specimens were each tested using temperature profile 2. **Figure 6** shows both profiles along with the temperature data recorded for one of the samples (other samples similar) as well as the points at which warpage measurements were taken. Profile 1 begins with generic reflow heating, and after peaking at 225°C, the sample cools naturally to 100°C. The specimen is then reheated to a second 225°C peak followed by a complete natural cooldown to room temperature. Cooling and reheating at 100°C was performed to drive off any residual moisture on the board, and observe any associated warpage change. One complete cycle lasted approximately 90 minutes. Profile 2 is a gradual heating cycle implemented for the purpose of FEA warpage model validation. The peak temperature (130°C) is set below the  $T_g$  of the organic core material so that the models only need to address elastic behavior.

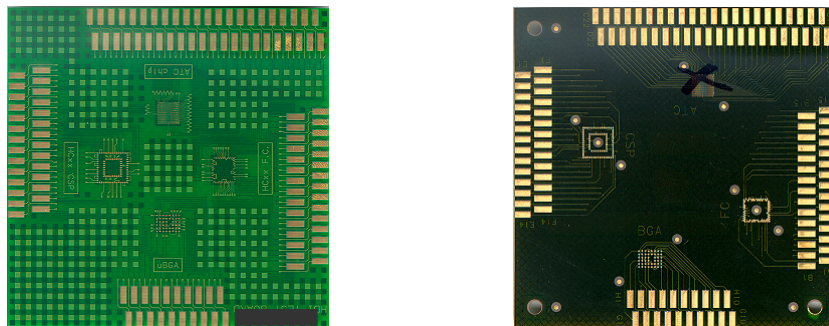


**Figure 5:** Light Green and Dark Green HDI Test Vehicles

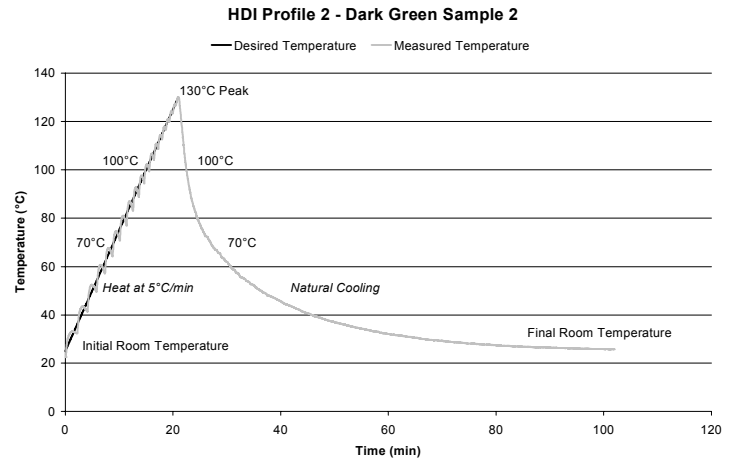
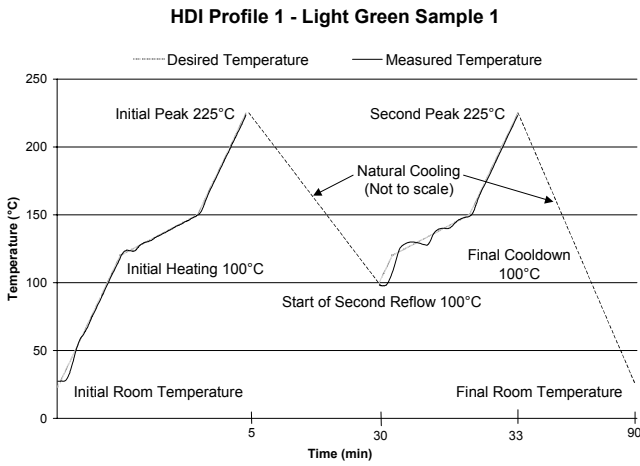


**Figure 6.** HDI Profiles 1 and 2

## EXPERIMENTAL RESULTS

Selected results from all the measurements performed are shown in **Figures 8 - 27**. Each figure includes the observed fringe pattern, 9-point warpage values, and three-dimensional surface plot. To follow changes at known points, specific warpage data is given at locations along the board perimeter and center (see **Figure 7** for positions). The first warpage measurement for each of the samples is given as absolute warpage, obtained during the initial measurement made at room temperature. Values are normalized such that the lowest point measured is set equal to zero. Subsequent plots are then determined by subtracting the initial master reference (room temperature warpage) from the current measurement; hence, results are given relative to the original shape of the board and are referred to as relative warpage. The “Warpage Across Specimen” value reported beneath each plot is the maximum absolute warpage measured and effectively represents the overall flatness of the specimen. **Tables 1 and 2** lists these values for all the samples.

| Profile Point        | Warpage Across Specimen |            |
|----------------------|-------------------------|------------|
|                      | Lt Green 1              | Dk Green 1 |
| Initial Room Temp.   | 14.0                    | 29.3       |
| Heating (100°C)      | 8.1                     | 20.6       |
| Initial Peak (225°C) | 14.1                    | 19.0       |
| Cooling (100°C)      | 20.1                    | 12.4       |
| Second Peak (225°C)  | 14.8                    | 19.4       |
| Cooling (100°C)      | 20.9                    | 12.3       |
| Final Room Temp.     | 19.6                    | 30.0       |

**Note:** Units are in mils.

**Table 1:** Warpage Data Summary for Lt Green Sample 1 and Dk Green Sample 1 Tested Under Profile 1

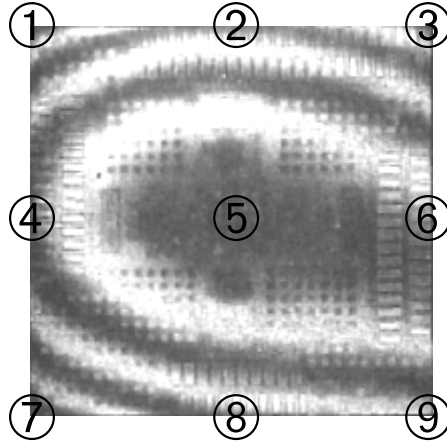


**Figure 7.** 9-Point Locations (Values given in mils)

#### *Effect of Moisture on Warpage*

Light green sample 1 and dark green sample 1 were tested using profile 1. The light green specimen was initially shaped concave down with a warpage of 14 mils, and had a symmetric fringe pattern (**Figure 8**). After heating to 100°C, the board experienced a flattening of approximately 6 mils, with the horizontal centerline sagging. Once at the initial peak temperature of 225°C (**Figure 10**), the sample demonstrated a warpage increase back to approximately 14 mils; small twisting deflections were present along the top and bottom edges. When cooling off to 100°C, the sample closely resembled its initial symmetric shape with an additional increase in warpage to 20 mils. Once the specimen is reheated back to 225°C, it effectively returned to the shape and magnitude seen at the first peak (**Figure 12**). Again, the board warped symmetrically after cooling to 100°C a second time, with practically identical shape and flatness when previously at this temperature. There is little change when the sample was cooled to final room temperature (**Figure 14**); warpage was symmetrical and concave down, showing approximately a six mil decrease in overall flatness with final warpage across the specimen at nearly 20 mils.

Dark green specimen 1 had an initial upward concavity with approximately twice as much warpage as the light green sample at 29.3 mils (**Figure 9**); again the fringe pattern was completely symmetric. Upon heating to 100°C, the sample flattened nearly 10 mils. Then at the first peak temperature, (**Figure 11**) the specimen decreased in warpage even further to 19 mils having a horseshoe-shaped fringe pattern with extremities found at the top and bottom edges. Flattening continued as the sample cooled to 100°C and warpage decreased to 12.4 mils as fringes surrounded the top and right edge pads. After being reheated to 225°C (**Figure 13**), the sample closely resembled its state at the previous peak temperature. When the specimen is cooled to 100°C a second time, it had the practically identical

shape and flatness (12.3 mils) when previously at this temperature. The same trend holds true for the final room temperature measurement (**Figure 15**). The sample returned to its pre-heated state, but with a slightly flatter bottom edge.

Comparison of these results shows that both specimens demonstrate repeatable results under repeated temperature conditions, specifically at 225°C peak heating 100°C cooldown. It is obvious that moisture has an effect on warpage, as seen from the data listed in **Table 1**. Any moisture present is driven away upon initial heating (100°C) of the specimens, where warpage decreases from initial room temperature values. Warpage at the subsequent 100°C cooling points is nearly equal for each specimen (Lt green: 20.1 and 20.9, dk green: 12.4 and 12.3, respectively) but different than the initial 100°C warpage. In addition, the dark green sample shows an overall warpage change (18 mils) three times as great as the light green (6 mils) but finishes with nearly the same initial warpage unlike the light green specimen (6 mil increase).

| Profile Point        | Warpage Across Specimen |            |            |            |
|----------------------|-------------------------|------------|------------|------------|
|                      | Lt Green 2              | Lt Green 3 | Dk Green 2 | Dk Green 3 |
| Initial Room Temp.   | 15.2                    | 17.7       | 32.3       | 25.7       |
| Heating (70°C)       | 13.3                    | 17.6       | 14.1       | 9.8        |
| Heating (100°C)      | 12.5                    | 17.1       | 11.8       | 8.5        |
| Peak Heating (130°C) | 14.5                    | 14.0       | 10.2       | 10.3       |
| Cooling (100°C)      | 17.2                    | 18.6       | 12.7       | 11.0       |
| Cooling (70°C)       | 18.6                    | 19.9       | 14.8       | 12.5       |
| Final Room Temp.     | 19.9                    | 19.4       | 29.8       | 24.8       |

**Note:** Units are in mils.

**Table 2:** Warpage Data Summary for Lt Green Samples 2 & 3 and Dk Green Samples 2 and 3 Tested Under Profile 2

*Effect of Gradual Heating on Warpage*

The remaining two light green and dark green samples were tested using profile 2. Both light green samples began concave down at room temperature, with similar magnitudes at approximately 15 and 18 mils, respectively (**Figures 16 & 17**). When heated to 70°C, sample 2 flattened nearly 2 mils as sample 3 effectively remained unchanged. At 100°C, sample 2 flattened an additional mil to 12.5 mils while sample 3 again experienced negligible change. Once at the peak temperature of 130°C (**Figures 18 & 19**), both specimens were near equal in overall warpage at approximately 14 mils, where specimen 2 displayed an uneven twisting while sample 3 exhibited a more symmetric flattening. Upon cooldown to 100° C and then 70°, both samples underwent a warpage increase with shapes similar to those seen when at peak heating. After completely cooling to final room temperature (**Figures 20 & 21**), the samples

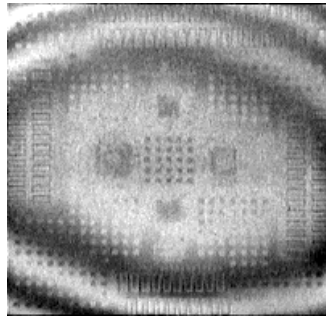
returned close to their original shapes with an increase from their initial readings, of approximately 19.5 mils.

The initial warpage of dark green samples 2 and 3 were concave up (**Figures 22 & 23**) with maximum warpage found at the samples' corners. The fringe pattern for sample 2 showed an upper left to lower right diagonal symmetry while sample 3 was symmetric about its vertical centerline. At 70°C, both samples flattened considerably along the same symmetric patterns and continued to decrease in warpage when heated to 100°C. Both samples were at even warpage magnitudes (~10 mils) during peak heating (**Figures 24 & 25**). The equal behavior seen at this temperature was a result of sample 2 flattening from 11.8 while sample 3 warped from 8.5 mils. The cooldown cycle brought on small steady warpage increases as the samples passed through 100°C and 70°C. When completely cooled to final room temperature (**Figures 26 & 28**), the specimens closely resembled their initial state, with both yielding a small overall decrease in warpage.

Comparison of the light and dark green sample results shows the light green samples less affected by the gradual heating. Although both light green specimens experience an overall increase in warpage, the maximum change at any time is less than 6 mils. In contrast, the dark green samples display some decrease in overall warpage and flatten even more than the light green during peak heating, but undergo significant warpage swings with magnitude changes as large as 22 mils. The dark green design also appears to be sensitive to immediate room temperature thermal transitions.

The thermo-mechanical behavior of an HDI assembly largely influences its design parameters. Since HDI boards are inherently thinner than their conventional counterparts, they are more susceptible to thermally-induced warpage. HDI technology allows the redesigning of current double-sided boards into smaller, thinner single-sided versions, typically with an asymmetrical internal layering. Due to this uneven layer distribution, HDI assemblies are more likely to experience solder mask cracking caused by relatively large internal assembly stresses. Aside from the manufacturing advantages of processing single-sided product, HDI may still need to be thicker than theoretically necessary to balance layering to keep warpage behavior at an acceptable level. Measurement data from these few samples suggests that a relatively thicker HDI is an overall “better” warpage performer. During high heat processing of thinner HDI assemblies, it is possible that HDI fabricators may require board fixturing (temporary stiffening supports). More uniform convective heating will most likely reduce temperature gradient-related warpage brought on by uneven IR heating.

These measurements help give HDI designers some insight into understanding overall warpage performance. The results collected here were used specifically to validate FEA warpage models which were used only to predict optimum HDI manufacturing processing temperatures. Further tests and models



(a)

| 9 Point Absolute Warpage |       |       |
|--------------------------|-------|-------|
| 2.06                     | 5.86  | 0.02  |
| 11.87                    | 13.79 | 11.25 |
| 3.31                     | 7.91  | 6.73  |

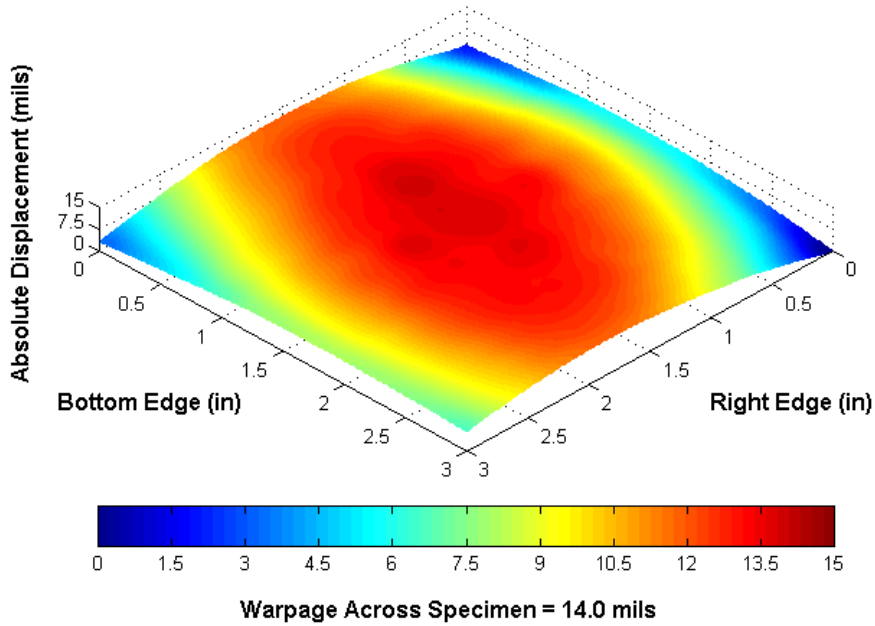
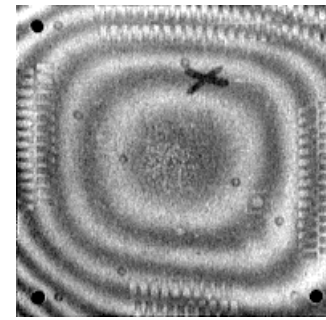


**Figure 8:** Light Green Specimen 1 at Initial Room Temperature  
 (a) Moiré Pattern, (b) Point Values, (c) 3-D Surface Plot



(a)

| 9 Point Absolute Warpage |       |       |
|--------------------------|-------|-------|
| 23.21                    | 17.11 | 25.03 |
| 13.90                    | 0.57  | 11.85 |
| 29.26                    | 16.09 | 15.68 |

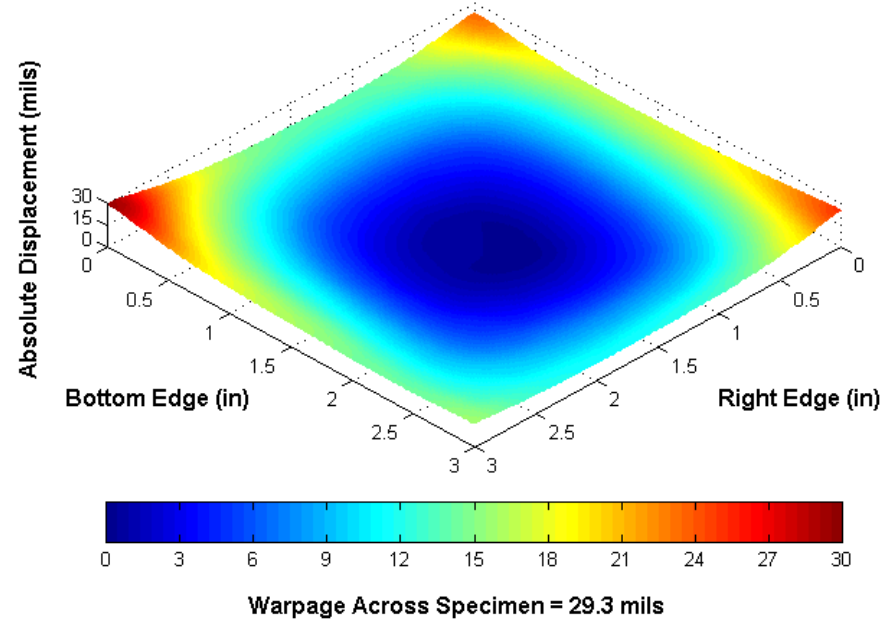
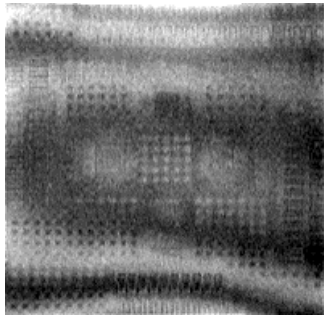


**Figure 9:** Dark Green Specimen 1 at Initial Room Temperature  
 (a) Moiré Pattern, (b) Point Values, (c) 3-D Surface Plot

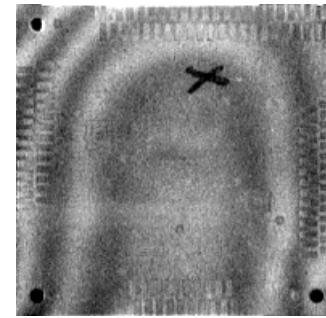
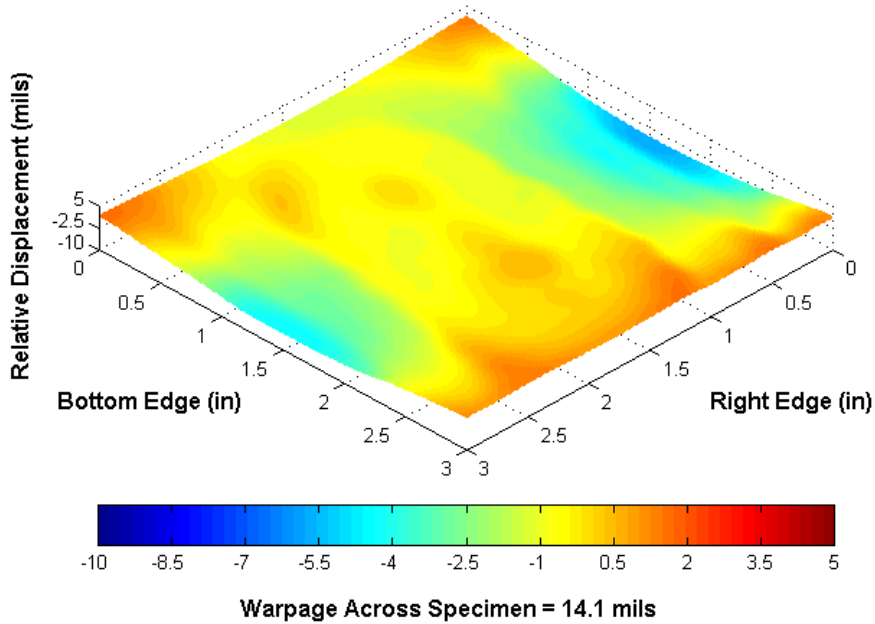


(a)

*Warpage Change at 9 Points*

|       |       |      |
|-------|-------|------|
| 1.4   | -5.73 | 1.19 |
| -1.11 | -0.41 | 1.17 |
| 1.63  | -4.34 | 1.13 |

(b)



(a)

*Warpage Change at 9 Points*

|        |        |        |
|--------|--------|--------|
| -4.16  | -9.19  | -11.77 |
| -2.57  | 0.87   | -1.90  |
| -19.21 | -16.06 | -4.27  |

(b)

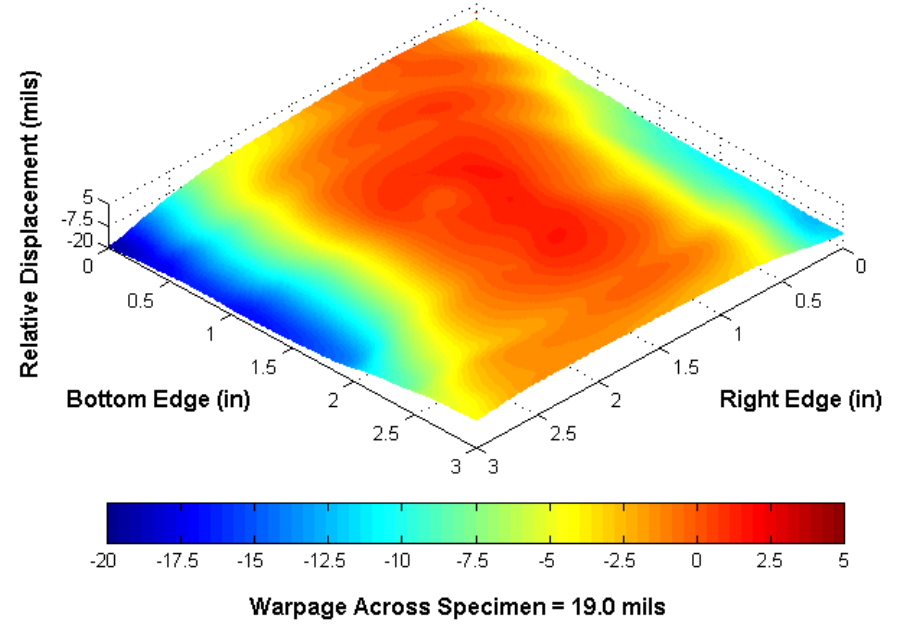
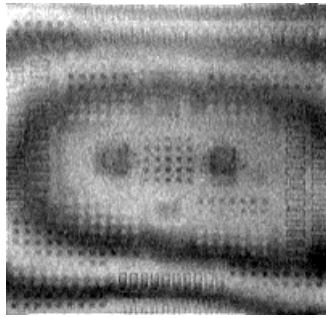


**Figure 10:** Light Green Specimen 1 at Initial Peak Heating 225°C  
 (a) Moiré Pattern, (b) Point Values, (c) 3-D Surface Plot

**Figure 11:** Dark Green Specimen 1 at Initial Peak Heating 225°C  
 (a) Moiré Pattern, (b) Point Values, (c) 3-D Surface Plot



(a)

| Warpage Change at 9 Points |       |      |
|----------------------------|-------|------|
| 0.85                       | -5.55 | 0.67 |
| -1.72                      | 0.21  | 0.79 |
| 0.36                       | -4.62 | 0.34 |

(b)

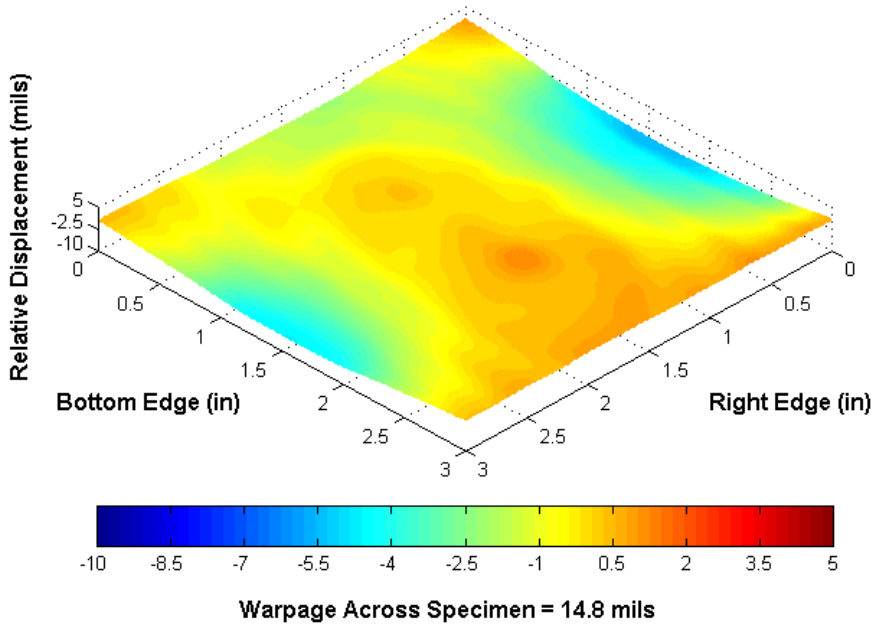
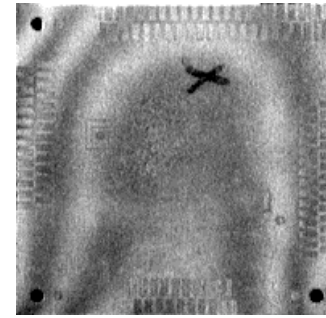


**Figure 12:** Light Green Specimen 1 at Second Peak Heating 225°C  
(a) Moiré Pattern, (b) Point Values, (c) 3-D Surface Plot



(a)

| Warpage Change at 9 Points |        |        |
|----------------------------|--------|--------|
| -3.85                      | -8.55  | -11.31 |
| -1.86                      | 4.59   | -0.58  |
| -18.57                     | -15.98 | -2.93  |

(b)

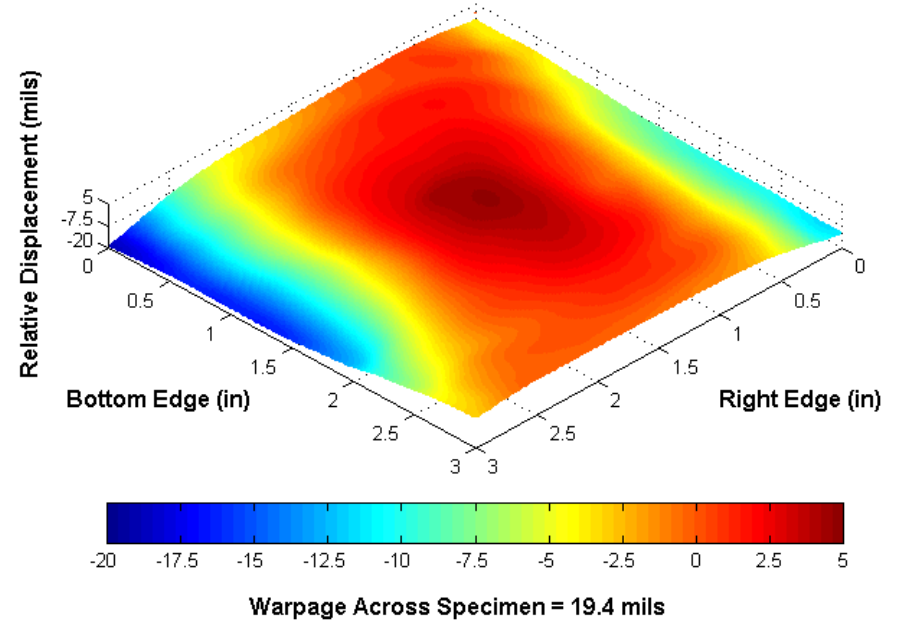
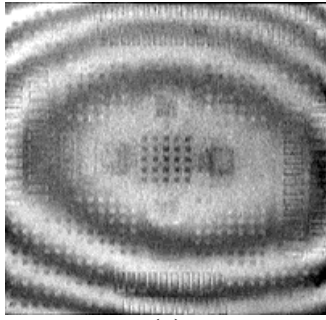


**Figure 13:** Dark Green Specimen 1 at Second Peak Heating 225°C  
(a) Moiré Pattern, (b) Point Values, (c) 3-D Surface Plot



(a)

| Warpage Change at 9 Points |      |      |
|----------------------------|------|------|
| -0.18                      | 1.24 | 0.01 |
| 2.16                       | 5.76 | 4.67 |
| 0.18                       | 0.63 | 0.06 |

(b)

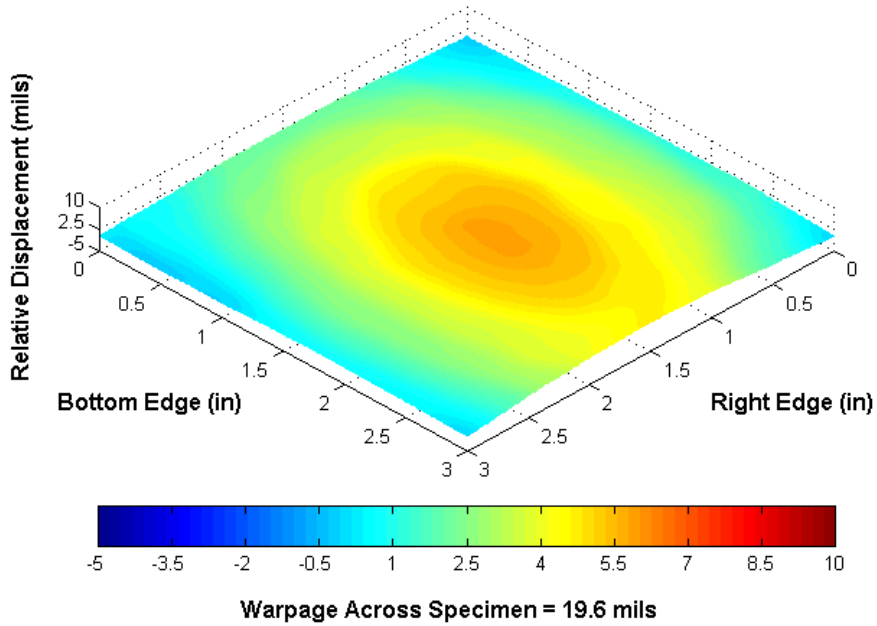
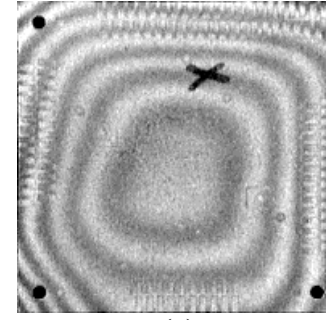


**Figure 14:** Light Green Specimen 1 at Final Room Temperature  
(a) Moiré Pattern, (b) Point Values, (c) 3-D Surface Plot



(a)

| Warpage Change at 9 Points |       |      |
|----------------------------|-------|------|
| 6.77                       | 6.62  | 2.54 |
| 3.97                       | 0.39  | 5.39 |
| -2.50                      | -6.20 | 3.70 |

(b)

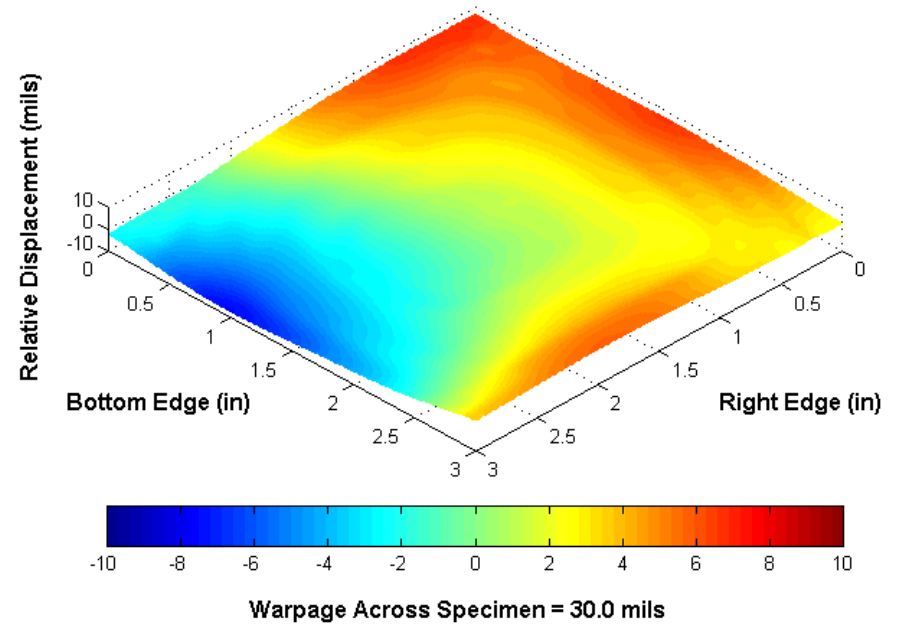
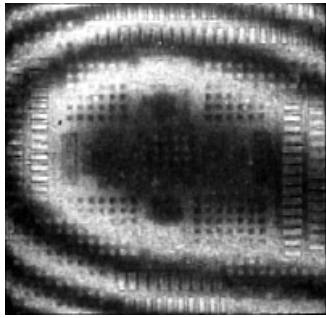


**Figure 15:** Dark Green Specimen 1 at Final Room Temperature  
(a) Moiré Pattern, (b) Point Values, (c) 3-D Surface Plot



(a)

| 9 Point Absolute Warpage |       |       |
|--------------------------|-------|-------|
| 1.02                     | 5.79  | 1.44  |
| 10.77                    | 15.05 | 13.74 |
| 0.00                     | 6.17  | 7.83  |

(b)

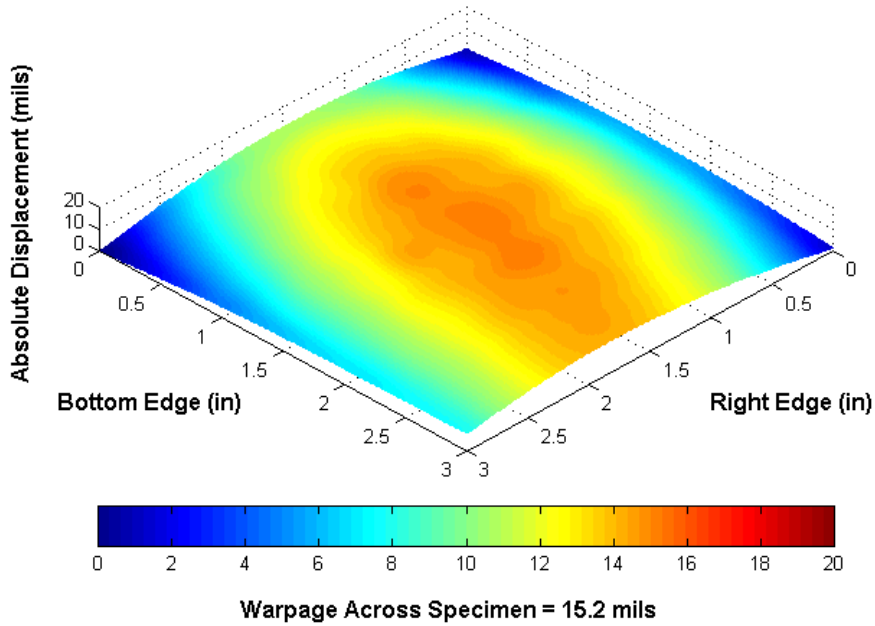
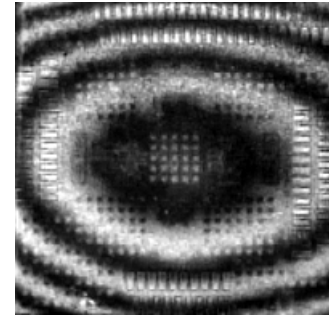


**Figure 16:** Light Green Specimen 2 at Initial Room Temperature  
(a) Moiré Pattern, (b) Point Values, (c) 3-D Surface Plot



(a)

| 9 Point Absolute Warpage |       |       |
|--------------------------|-------|-------|
| 0.02                     | 4.78  | 0.63  |
| 12.45                    | 17.69 | 13.75 |
| 0.22                     | 7.30  | 4.10  |

(b)

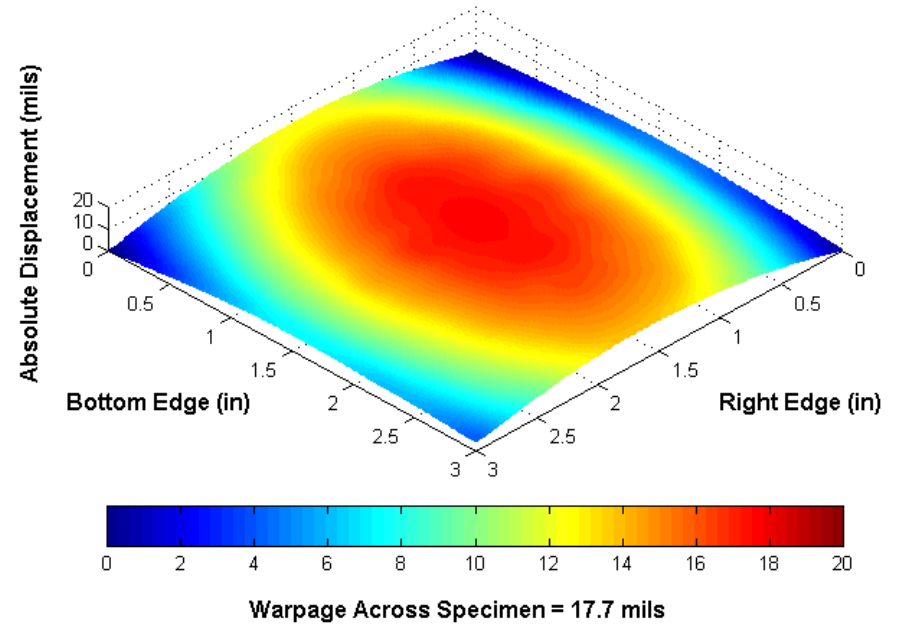
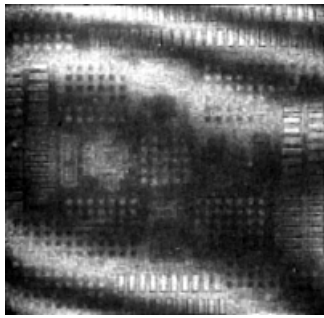


**Figure 17:** Light Green Specimen 3 at Initial Room Temperature  
(a) Moiré Pattern, (b) Point Values, (c) 3-D Surface Plot



(a)

| Warpage Change at 9 Points |       |       |
|----------------------------|-------|-------|
| 4.97                       | -1.63 | -1.43 |
| 2.54                       | -1.62 | -1.09 |
| 4.56                       | 2.42  | 4.65  |

(b)

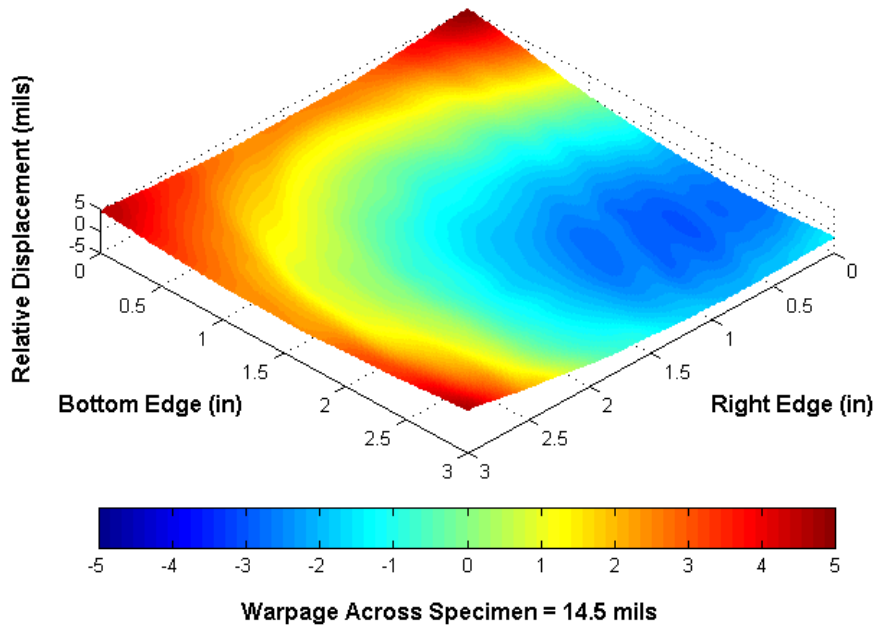
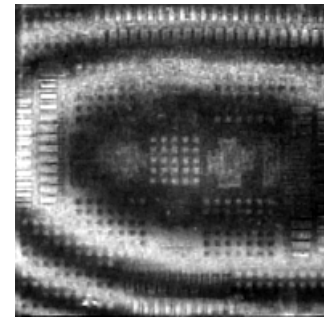


**Figure 18:** Light Green Specimen 2 at Peak Heating 130°C  
(a) Moiré Pattern, (b) Point Values, (c) 3-D Surface Plot



(a)

| Warpage Change at 9 Points |       |       |
|----------------------------|-------|-------|
| 2.21                       | -0.60 | 2.43  |
| -2.09                      | -3.85 | -1.00 |
| -0.21                      | -2.17 | 1.93  |

(b)

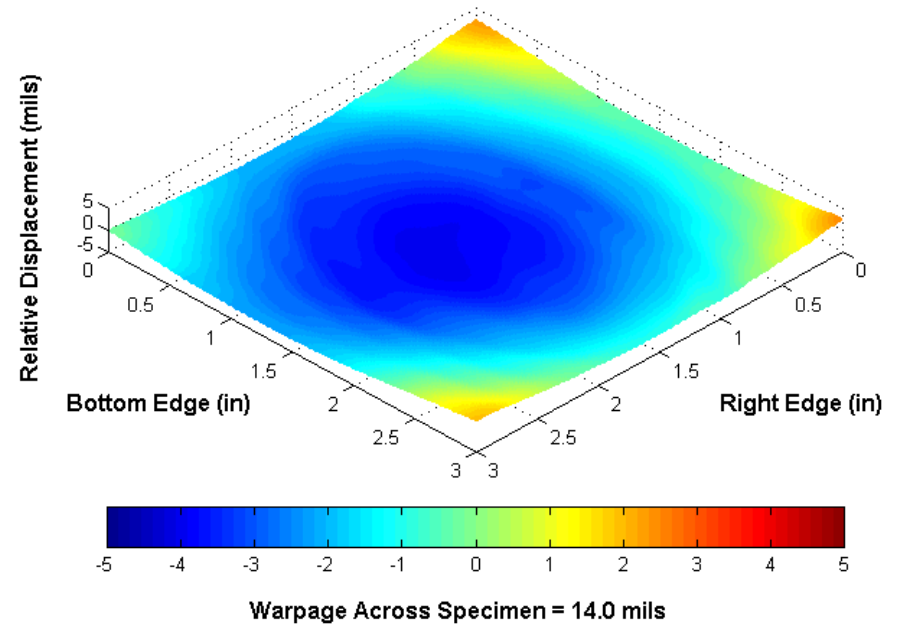
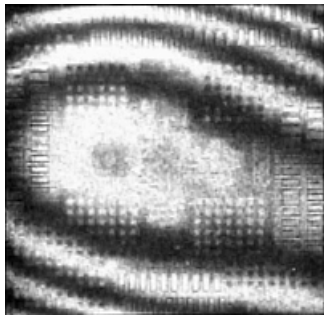


**Figure 19:** Light Green Specimen 3 at Peak Heating 130°C  
(a) Moiré Pattern, (b) Point Values, (c) 3-D Surface Plot



(a)

| <i>Warpage Change at 9 Points</i> |      |       |
|-----------------------------------|------|-------|
| 4.93                              | 1.96 | -1.42 |
| 5.65                              | 3.54 | 2.33  |
| 4.58                              | 4.61 | 5.14  |

(b)

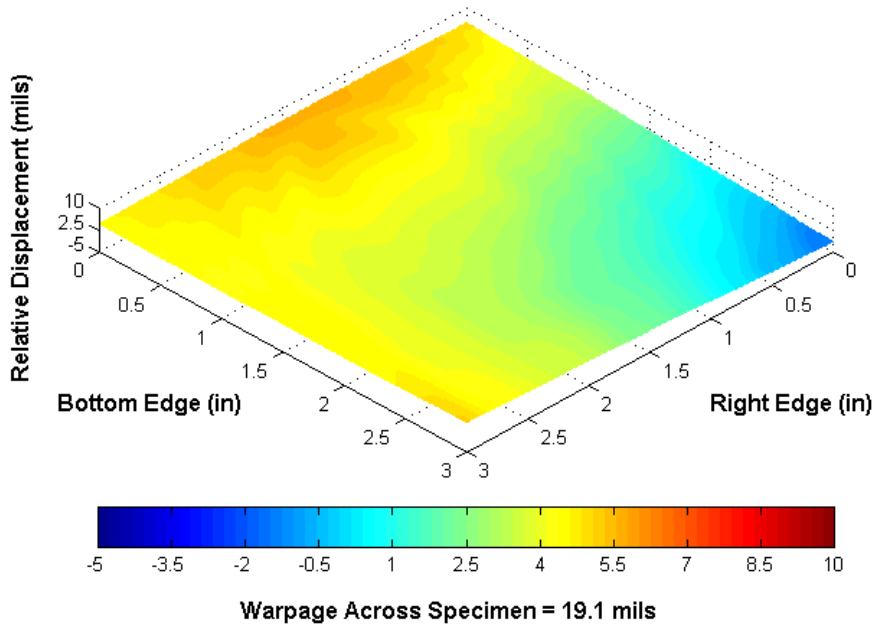
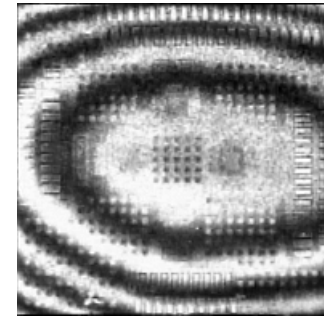


**Figure 20:** Light Green Specimen 2 at Final Room Temperature  
(a) Moiré Pattern, (b) Point Values, (c) 3-D Surface Plot



(a)

| <i>Warpage Change at 9 Points</i> |      |      |
|-----------------------------------|------|------|
| 2.75                              | 2.56 | 3.34 |
| 1.44                              | 1.59 | 2.97 |
| -0.21                             | 1.05 | 2.82 |

(b)

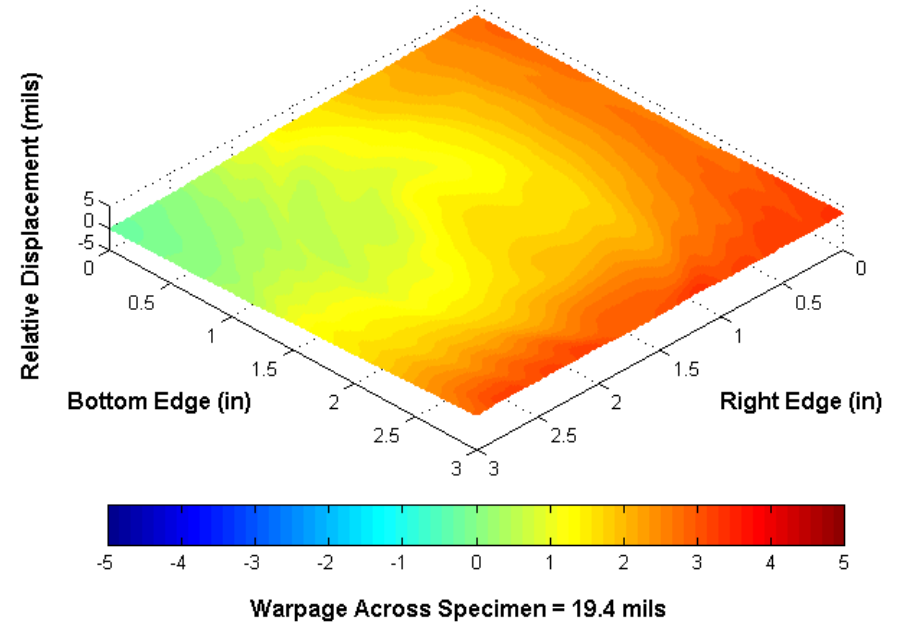
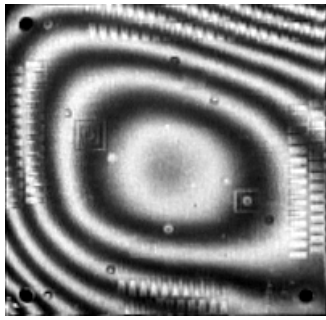


**Figure 21:** Light Green Specimen 3 at Final Room Temperature  
(a) Moiré Pattern, (b) Point Values, (c) 3-D Surface Plot



(a)

| 9 Point Absolute Warpage |       |       |
|--------------------------|-------|-------|
| 17.75                    | 18.68 | 32.30 |
| 13.90                    | 0.13  | 8.24  |
| 29.88                    | 13.78 | 9.83  |

(b)

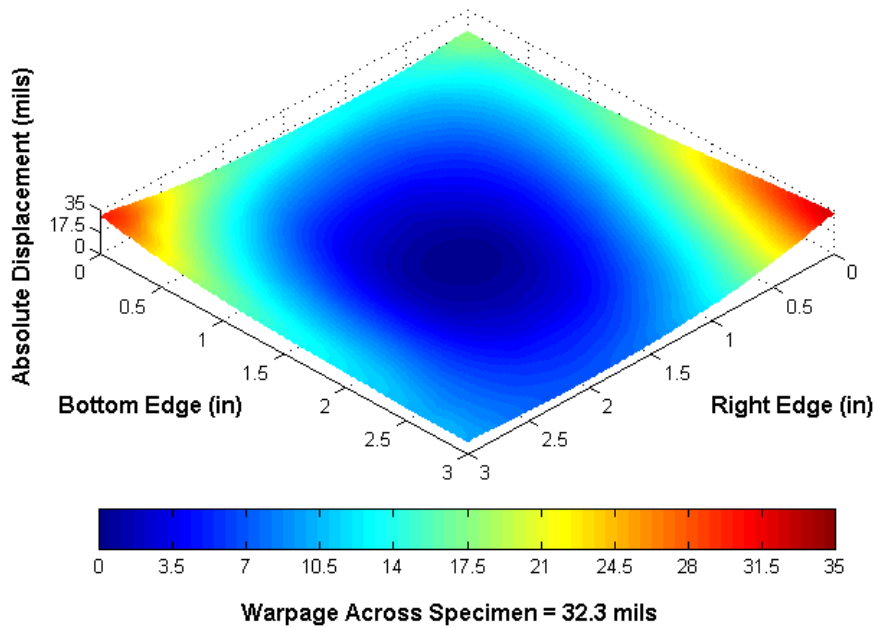
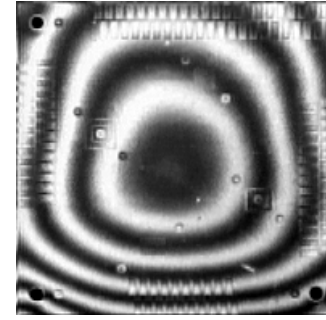


**Figure 22:** Dark Green Specimen 2 at Initial Room Temperature  
(a) Moiré Pattern, (b) Point Values, (c) 3-D Surface Plot



(a)

| 9 Point Absolute Warpage |       |       |
|--------------------------|-------|-------|
| 16.29                    | 9.25  | 18.16 |
| 12.21                    | 0.15  | 12.92 |
| 25.61                    | 16.87 | 21.76 |

(b)

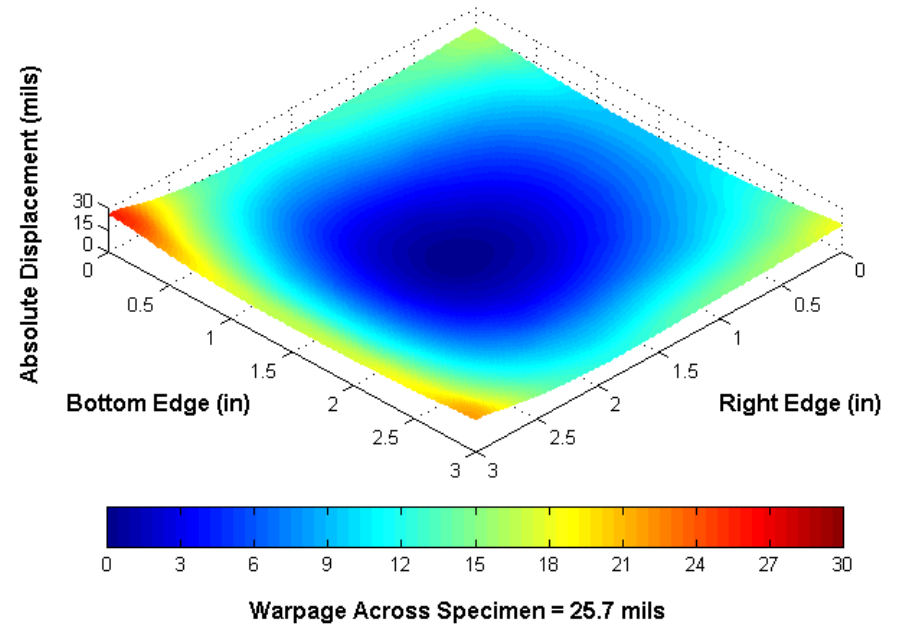
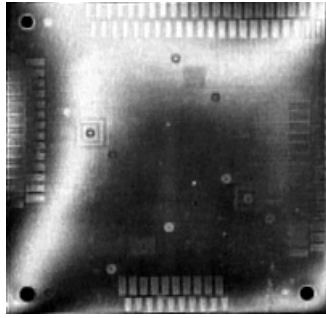


**Figure 23:** Dark Green Specimen 3 at Initial Room Temperature  
(a) Moiré Pattern, (b) Point Values, (c) 3-D Surface Plot



(a)

*Warpage Change at 9 Points*

|        |        |        |
|--------|--------|--------|
| -9.72  | -12.10 | -26.20 |
| -4.06  | 3.45   | -4.71  |
| -24.23 | -12.29 | -9.83  |

(b)

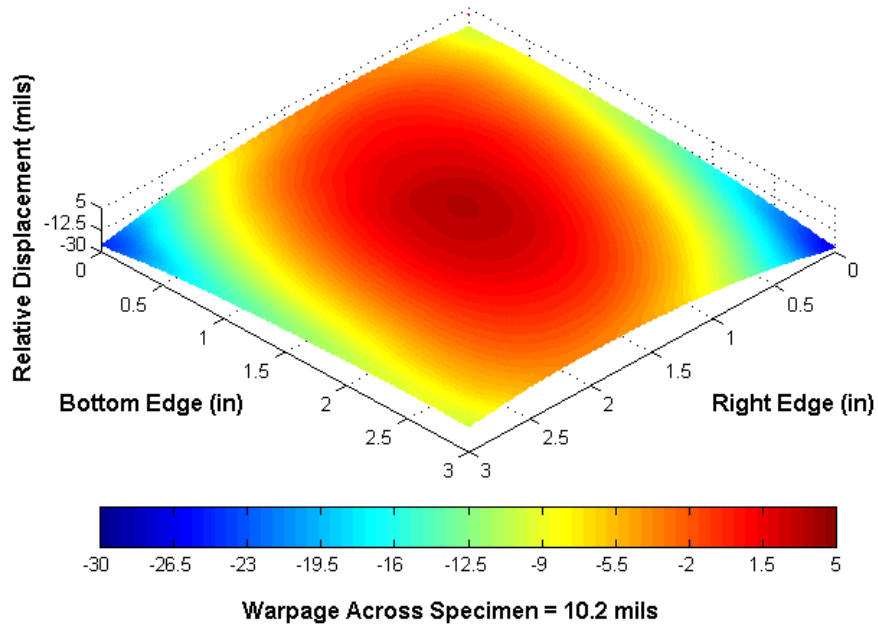
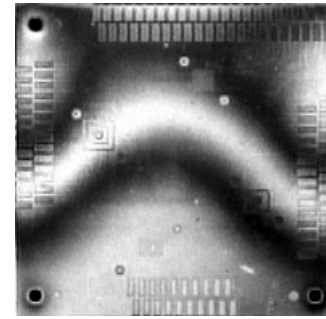


**Figure 24:** Dark Green Specimen 2 at Peak Heating 130°C  
 (a) Moiré Pattern, (b) Point Values, (c) 3-D Surface Plot



(a)

*Warpage Change at 9 Points*

|        |        |        |
|--------|--------|--------|
| -7.55  | -3.04  | -9.75  |
| -5.05  | 3.15   | -4.61  |
| -23.88 | -16.60 | -19.80 |

(b)

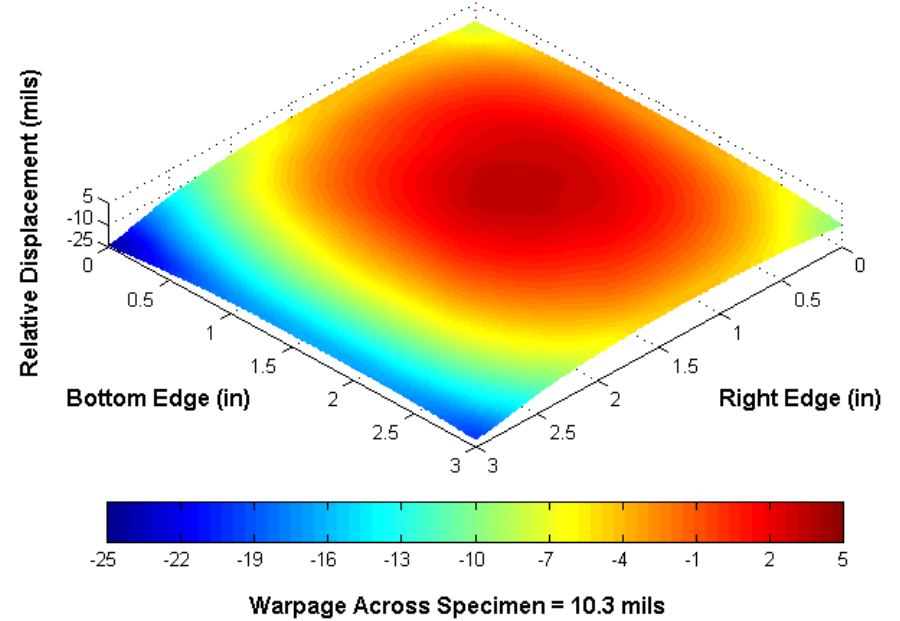
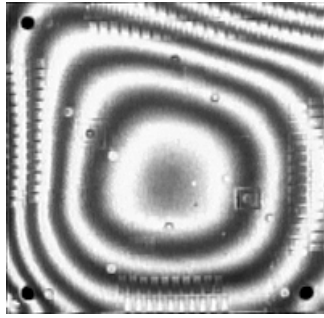


**Figure 25:** Dark Green Specimen 3 at Peak Heating 130°C  
 (a) Moiré Pattern, (b) Point Values, (c) 3-D Surface Plot



(a)

| Warpage Change at 9 Points |       |       |
|----------------------------|-------|-------|
| 1.69                       | -0.30 | -2.48 |
| 5.02                       | 0.40  | 3.68  |
| -3.97                      | -2.31 | 7.70  |

(b)

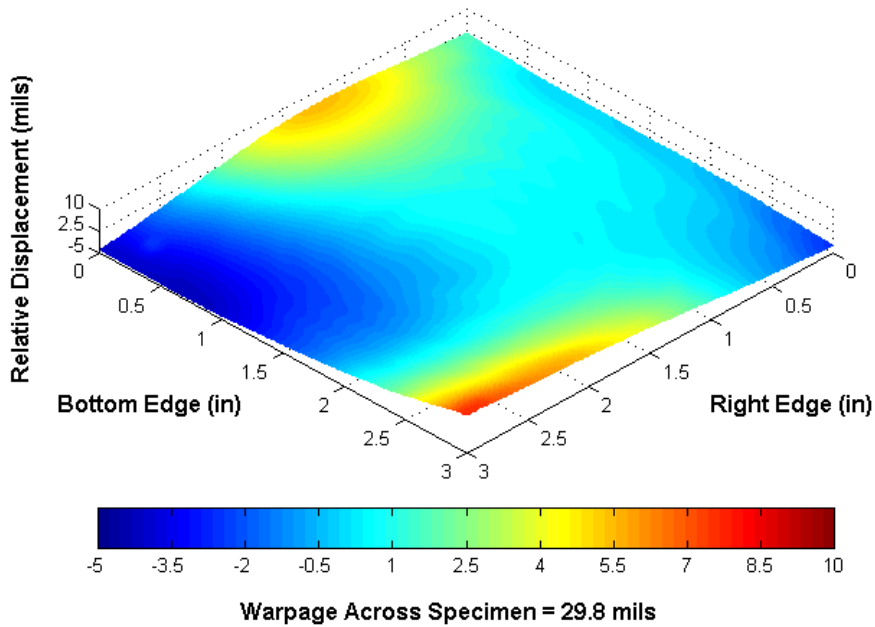
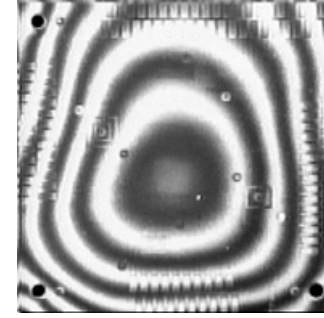


**Figure 26:** Dark Green Specimen 2 at Final Room Temperature  
(a) Moiré Pattern, (b) Point Values, (c) 3-D Surface Plot



(a)

| Warpage Change at 9 Points |       |       |
|----------------------------|-------|-------|
| 8.54                       | 0.66  | 3.22  |
| 4.81                       | 0.41  | 4.98  |
| -1.41                      | -3.59 | -0.15 |

(b)

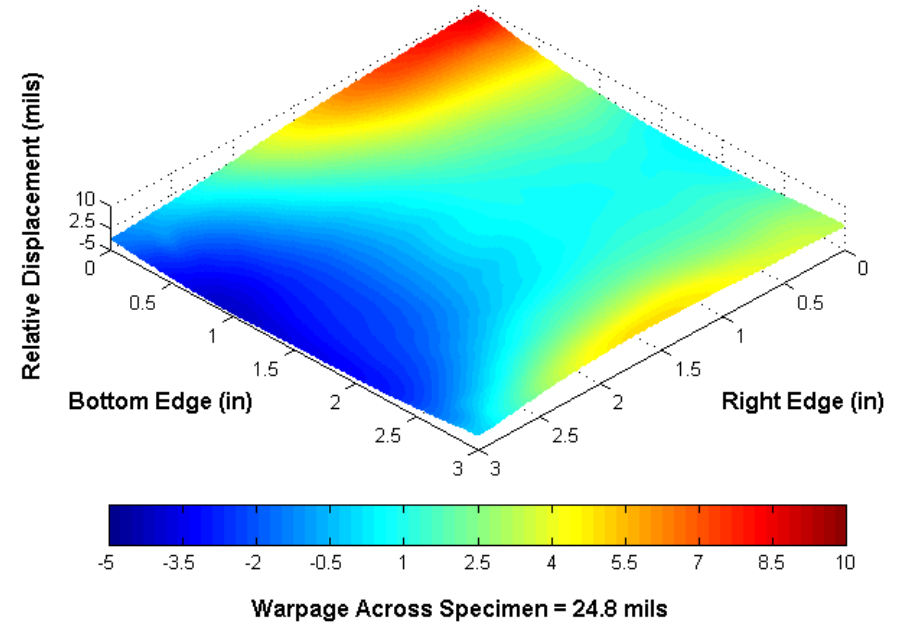


**Figure 26:** Dark Green Specimen 3 at Final Room Temperature  
(a) Moiré Pattern, (b) Point Values, (c) 3-D Surface Plot

could be developed to study the how other variables including layer composition, core material, and chip thickness affect HDI stiffness and warpage behavior.

## CONCLUSIONS AND FUTURE WORK

The many HDI options currently available to both PWB manufacturers and designers create a potential difficulty in choosing the specific methods to produce these products. However, final decisions will no doubt be influenced by many factors including cost, compatibility with existing equipment, and adequate warpage performance. Warpage measurement systems will be used for HDI PWBA design phase evaluations; if the evaluation is indicative of excessive warpage, design changes can be implemented before mass production.

The AEPL is working to expand its current capabilities of measuring thermally induced PWB warpage. Assembly of a new larger, more powerful oven with both convective and IR heating is underway. It will be equipped with projection and shadow moiré measurement systems having sub-mil range resolution. This system will be capable of measuring large area bare and populated boards up to 24" x 24" in size as well as small-scale specimens including ball grid arrays and multichip modules. New features will include computer-controlled specimen orientation, direct-to-disk automated image capturing, and real-time display of 3-D warpage at any desired temperature.

## ACKNOWLEDGEMENTS

The authors would like to thank DARPA for providing funding for this research under BAA 96-16. Our sincere gratitude goes to Dan Radack, Lou Concha, and William Russell.

## REFERENCES

1. Holden, Happy, "PWB Build-Up Technologies: Smaller, Thinner and Lighter," *Proceedings of NEPCON West '96*, Vol. 3, Anaheim, CA pp 1460-1468.
2. Crum, Susan. "35 Years of Progress in Electronics Technology." *Electronic Packaging & Production* Aug 1996: 53-58.
3. McDermott, Brian J. "Photodefined Via PCB's Breaking the Design Rules." *Proceedings of NEPCON West '96*, Vol. 3, Anaheim, CA pp. 1480-1486.
4. Y. Wang and P. Hassel, "On-Line Measurement of Thermally Induced Warpage of BGAs with High Sensitivity Shadow Moiré," *International Journal of Microcircuits and Electronic Packaging*, Issue II, Vol. 21, No.2, 1998.

5. Y. Wang and P. Hassel, "Measurement of Thermally Induced Deformation of a BGA Using Phase-Stepping Shadow Moiré," *Experimental/Numerical Mechanics in Electronic Packaging*, Vol. 2, pp.32-39, 1998.
6. M. Stiteler and C. Ume, "System for Real-Time Measurements of Thermally Induced Warpage in a Simulated Infrared Soldering Environment," *ASME Journal of Electronic Packaging*, Vol. 119, pp. 1-7, 1997.
7. M. Stiteler, C. Ume and B. Leutz, "In-Process Board Warpage Measurement in a Lab Scale Wave Soldering Oven," *IEEE Transactions on Components, Packaging, and Manufacturing Technology*, Part A, Vol. 19, pp. 562-569, 1996.
8. Kobayashi, A. ed., *Handbook on Experimental Mechanics*, Prentice Hall, NJ 1987, pp. 282-313.